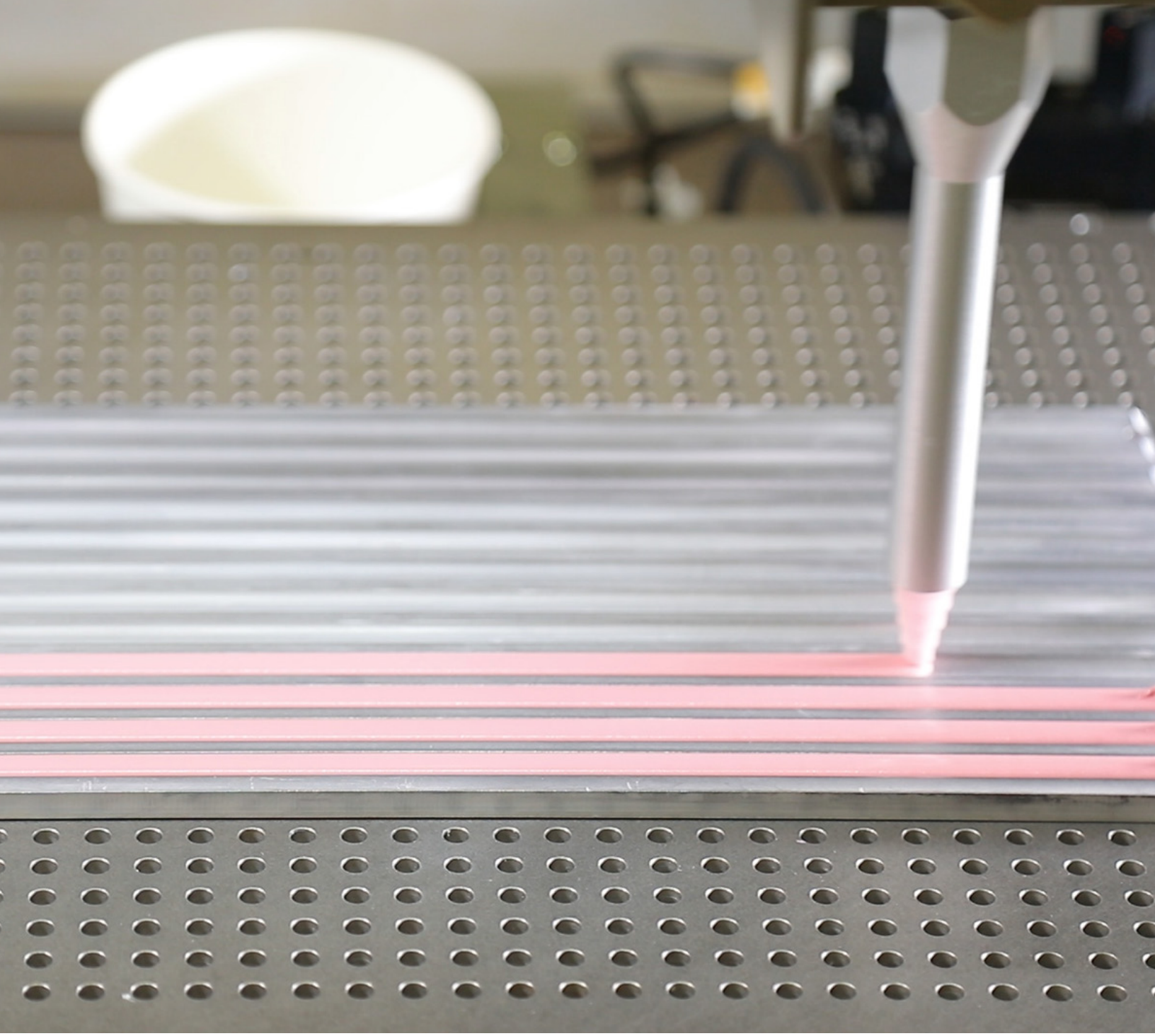

Battery Cooling Performance

Comparing Liquid-Dispense Gap Fillers with Thermal Pads
White Paper

Parker LORD

ENGINEERING YOUR SUCCESS.

Battery Cooling Performance

Comparing Liquid-Dispense Gap Fillers with Thermal Pads

Dr. Daniel Barber - Staff Scientist II

Eric Wyman - Lead Global Applications Engineer

Abstract

A study is conducted to compare thermal performance in battery modules using different thermal interface materials (TIMs) to connect the battery cells to a cooling plate. CoolTherm® liquid-dispense gap fillers are compared with thermal gap pads of comparable thermal conductivity. The gap fillers are shown to remove more heat from the batteries and provide lower battery temperatures than the gap pads. Furthermore, the gap fillers can provide the same benefit even when manufacturing tolerances are simulated, whereas gap pads perform significantly worse in these cases.

Introduction

A previous Parker LORD white paper described the use of CoolTherm liquid-dispensed, cure-in-place gap fillers as thermal interface materials (TIMs) for high power density battery packs for electric vehicles (EVs).[1] In that paper, we compared the thermal impedance of gap fillers with that of commercially-available gap pads of similar thermal conductivity and thickness. As described in that white paper, the surface roughness between the two contacting surfaces (for example, between a battery cell or module and the cooling plate) leads to only a small fraction of the apparent surfaces coming in direct contact with one another, thereby entrapping air.

[1] *T. Fornes et al., Liquid-Dispense Gap Fillers vs. Thermal Pads: A Case Study on Thermal Performance, https://www.lord.com/products-and-solutions/electronic-materials/thermal-management-materials/gap-fillers-vs-thermal-pads*

Our key finding was that Parker LORD liquid-dispense gap fillers provide lower thermal impedance than thermal pads having comparable bulk thermal conductivity and thickness, according to a steady-state thermal analysis. This result was largely due to the ability of the gap filler to readily conform to microscopically rough surfaces of the adjoining substrates (see Figure 1), which greatly lowers the interfacial impedance. This conformability effect was found to be quite pronounced in that the thermal impedance of CoolTherm SC-1200 gap filler, with thermal conductivity of 2 W/m·K, at 1mm thickness was comparable to a thermal pad with thermal conductivity of 4 W/m·K.

The focus of this white paper is to investigate how the superior thermal transfer provided by gap fillers versus gap pads affects cooling of actual battery modules. Battery modules

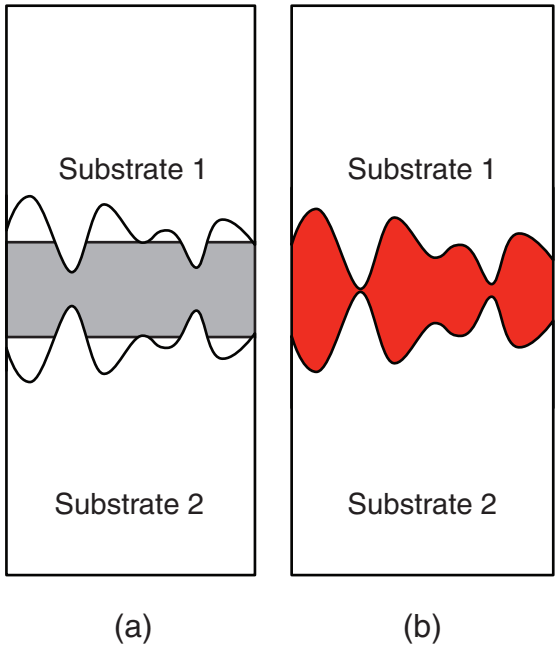

Figure 1: Illustration of the lack of microscopic conformability of solid thermal pads (left) relative to liquid-dispense gap fillers (right)

were assembled using Parker LORD gap fillers with thermal conductivity of 2 and 4 W/m·K, and also with commercially available gap pads of the same nominal thermal conductivity. The degree of cooling for each assembled module was then measured during a fast-charging cycle. The work confirms that the Parker LORD gap fillers provide superior battery cooling compared to the gap pads.

The previous white paper also predicted that the conformability effect would apply to assembled battery modules, in that gap fillers would more easily fill in gaps between the cells and the cooling plate that result from manufacturing tolerances. Tolerance of manufactured parts is specified by the customer, with tighter tolerance leading to more costly modules and packs. With large-form battery packs, the tolerance from uneven metal surfaces due to welding or fixturing, as well as stack-up tolerances in making the modules, can create a large variance in the volume that needs to be occupied by the TIM. Liquid-dispense gap fillers allow for infinite patterns and volumes to fill all of the gaps, whereas thermal pads are limited by their thickness and mechanical hardness. Figure 2 illustrates this effect.

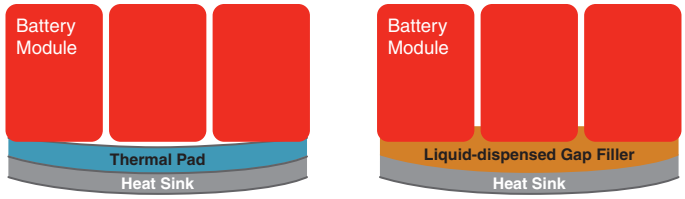

Figure 2: The effect of variable bond line thickness on the conformability of thermal pads (left) versus liquid-dispense gap fillers (right)

Table 1: List of TIMs used in this study

Product	CoolTherm SC-1200	CoolTherm SC-1500	Thermal Pad 1	Thermal Pad 2
Supplier	Parker LORD		Company 1	
Product Form	Liquid-dispensed Gap Filler		Gap Pad	
Nominal Thickness (mm)	NA	NA	1	1
Shore Hardness	OO-85	OO-75	OO-45	OO-75
Reported[(a)] Thermal Conductivity (W/m·K)	2.0	3.8	2.0	4.0
Measured[(b)] Thermal Conductivity (W/m·K)	2.0	4.1	1.3	4.2
Measured[(b)] Interfacial Impedance (K·cm²/W)	1.9	0.8	4.3	4.1

(a) Reported by supplier on product technical data sheet
(b) Measured via ASTM D5470 as reported in previous white paper[1]

Experimental

Table 1 lists the gap filler and thermal pad TIMs used in this study along with key properties. The thermal gap pads were selected to have comparable thermal conductivity and hardness values to that of CoolTherm SC-1200 and SC-1500 cure-in-place liquid gap fillers. Gap pads with a thickness of 1 mm were used.

Parker LORD partnered with the National Renewable Energy Lab (NREL) in Denver, Colorado (USA), for assistance in test design and for manufacture and testing of cell modules. NREL recommended a five-cell module using Samsung SDI prismatic cells (94 A·hr, 4.1 V), the same cells as used in the BMW i3 electric vehicle. All cells were outfitted with thermocouples at the top left, middle, and bottom right of one face

(a) (b)

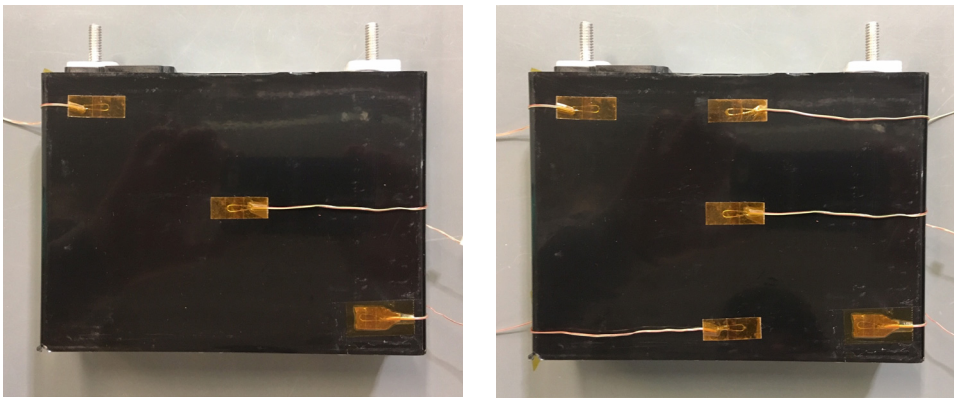

Figure 3: Placement of thermocouples on four of the battery cells (a) and additional thermal couples on the central battery cell (b)

(see Figure 3a). The central cell in the module had an additional two thermocouples at the top middle and bottom middle of the same face (see Figure 3b).

A liquid-cooled heat exchanger was attached to an aluminum plate coated to a thickness of 0.003 inch with a dielectric epoxy coating, LORD JMC-700K coating, with a thermally conductive paste (CoolTherm TC-404 grease, 4.3 W/m·K) between the metal layers. The cooling liquid was a 50/50 ethylene glycol/water mixture, with a volume flow rate controlled to within less than 1% variation by a positive displacement pump.

Figure 4: Assembly of battery cells onto cooling plate using a Parker LORD gap filler

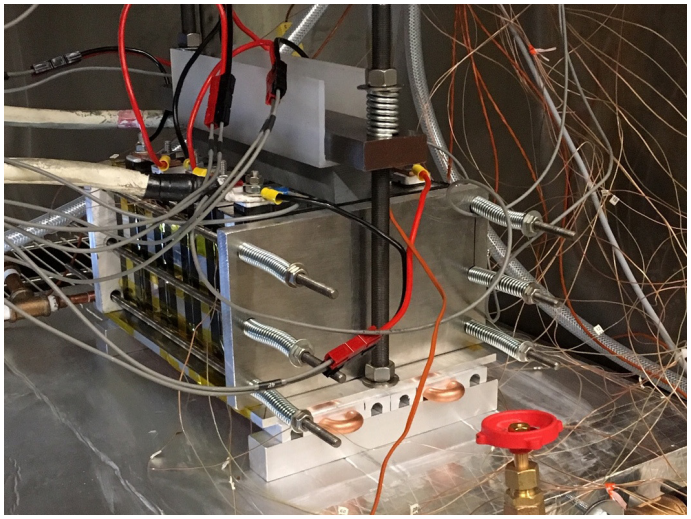

Figure 5: Fully-assembled cell module ready for thermal testing

Gap filler materials were dispensed onto the JMC-700K-coated plate (see Figure 4) and the five battery cells were pressed into the liquid gap filler, then clamped into place with a pressure of 4 psi from the sides and from above. Lexan shims of 1 mm thickness were used under the edges of the cells to provide an offset similar to the thickness of the gap pads used for the other modules. The gap fillers were then allowed to cure to solid form over 24 hours. For modules using gap pads, the pads were placed directly onto the cooling plate and the batteries were placed and clamped as above. For baseline modules, batteries were placed directly in contact with the dielectric-coated cooling plate.

To simulate manufacturing tolerance between the cells and the cooling plate observed in actual production battery modules, all modules were assembled either with or without additional 1-mm Lexan shims placed under the edges of cells #2 and #4. Baseline modules, with no thermal interface materials, were also assembled with and without shims. Constant pressure of 4 psi was used to press the cells together and also to press the cells down onto the cooling plate. A fully-assembled module is shown in Figure 5.

Cells were connected in series and charged using a 1.5C fast-charge cycle. Thermocouple temperatures and also inlet and outlet temperatures of the coolant liquid were monitored and recorded every 2 seconds during the charge cycle. Heat removed from the battery module by the coolant $P_{coolant}$, was determined from the mass flow rate $\dot{m}$, heat capacity of the coolant Cp, and the temperature difference of the outlet and inlet coolant ΔT, as in equation (1):

$$P_{coolant} = \dot{m}Cp\Delta T \quad (1)$$

Additionally, separate calorimetry measurements were conducted to determine the overall bulk temperature of the cell during operation. Tests were conducted in a drop calorimeter with no coolant flow to calculate the heat capacity of the battery module and to measure heat generation of the module during the 1.5C fast-charging cycle. The bulk temperature of the cells was then calculated at each time point after correcting for the power dissipated by the leads and by convection. Details of the calculations can be obtained upon request.

Results and Discussion

Thermal performance for the different modules was tested under fast-charging conditions. In this test, a constant current of 150A was applied until the voltage limit was reached, corresponding to 1.5C charge rate for our modules. Because the five cells were not completely electrically balanced during the charge event, it was necessary to apply lower levels of current for short time increments after the initial charge to reach 100% state-of-charge for the module. A typical charge cycle and the resulting voltage response are shown in Figure 6.

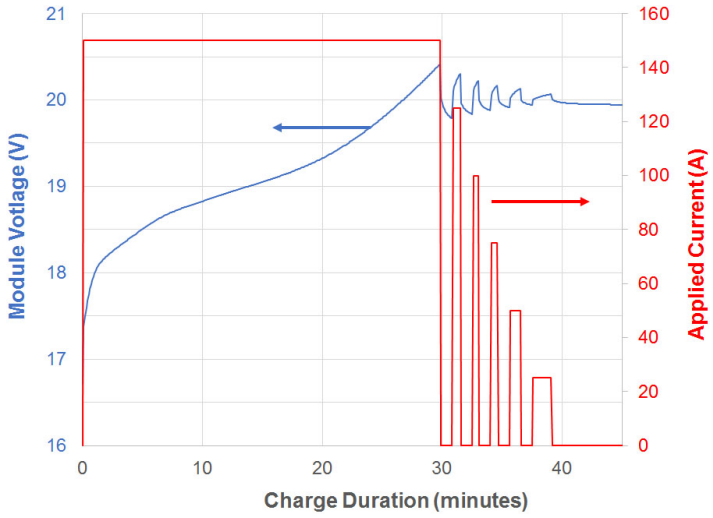

Figure 6: Fast-charging cycle showing current applied and resulting voltage response of the battery module

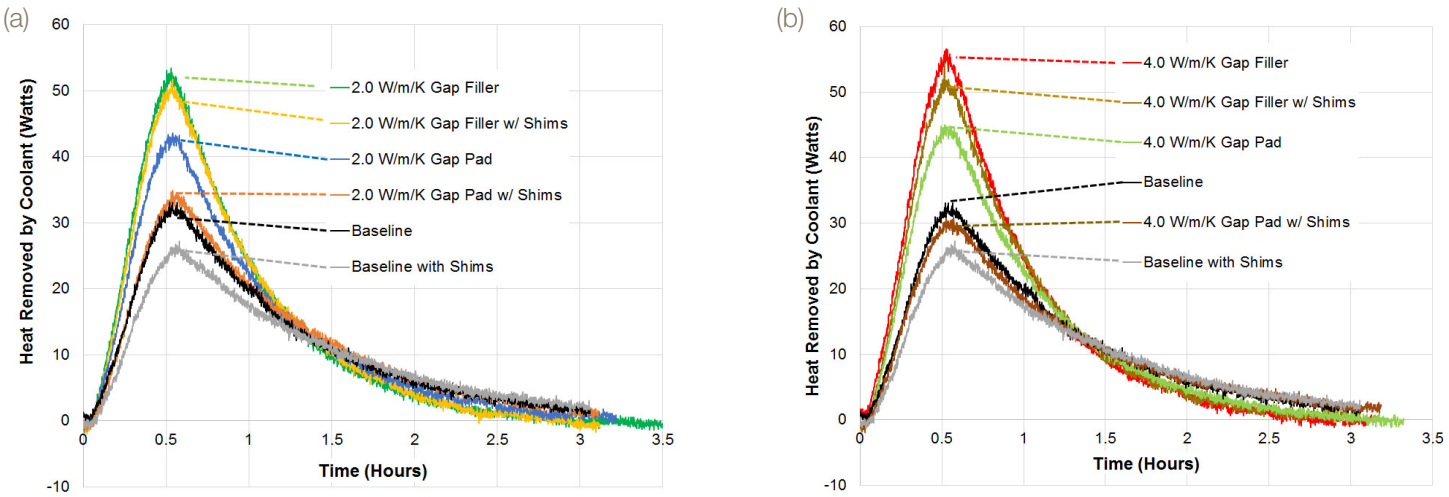

Figure 7: Comparison of heat removed from different module configurations by 2 W/m·K materials (a) and by 4 W/m·K materials (b). Baseline had no thermal interface material. Note that the legend order corresponds with the peak maximum for each material.

The total amount of heat removed from each module during the charging cycle was determined by measuring the increase in temperature of the cooling liquid at the outlet of the cooling plate and using this value, combined with the known coolant flow rate and heat capacity of the coolant, to calculate the power transferred to the coolant [refer to equation (1)]. These values are plotted versus time in Figures 7 and 8. A higher value of heat removed indicates a more efficient TIM and more cooling of the battery module.

Figure 7a compares CoolTherm SC-1200 gap filler (2 W/m·K) with the 2 W/m·K gap pad and with the baseline modules containing no TIM. Without simulating tolerance, the gap filler removes about 62% more heat than the baseline and about 24% more heat than the gap pad at the peak. With additional 1-mm shims at cells #2 and #4, the gap filler performance was barely affected, whereas the gap pad and baseline both decrease significantly. In this configuration, the gap filler removed twice as much heat as the baseline and about 47% more heat than the gap pad. This is likely due to the ability of the liquid-dispensed gap filler to conform to the irregularities in the cell-to-cooling plate distance, as predicted in our prior white paper (see Figure 2).

Figure 7b shows a similar comparison between CoolTherm SC-1500 gap filler (4 W/m·K) and the 4 W/m·K gap pad. Without additional shims, the gap filler removed nearly 70% more heat than the baseline and about 27% more heat than the gap pad at the peak. With additional shims the CoolTherm SC-1500 gap filler performed about the same as the 2 W/m·K gap filler, but the 4 W/m·K gap pad performed worse than both the 2 W/m·K gap pad with shims and the baseline without shims. We attribute this worse performance to the increased hardness of the 4 W/m·K gap pad, which prevents it from conforming to the uneven gaps between the individual battery cells and the cooling plate as well as the 2 W/m·K gap pad does. A similar effect was observed in our previous work, which showed that the thermal impedance of the 4 W/m·K gap pad was nearly the same as that of the

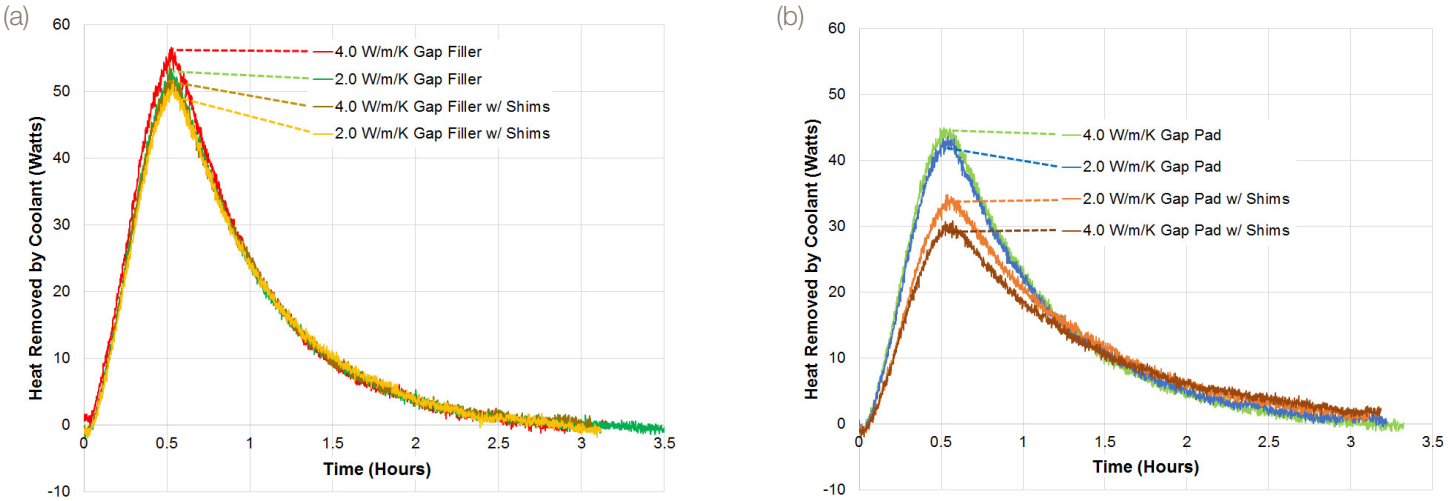

Figure 8: Comparison of heat removed by CoolTherm SC-1200 and SC-1500 (2 and 4 W/m·K, respectively) gap fillers (a) and by thermally conductive gap pads (b). Note that the legend order corresponds with the peak maximum for each material.

2 W/m·K gap pad (see Table 1) and was not improved as much by application of pressure due to its higher hardness.

Figure 8 shows the same data as in Figure 7, plotted to emphasize the comparison between thermally conductive materials of the same form. Figure 8a emphasizes the similarity in performance between the thermally conductive gap fillers, even when extra shims are present. By comparison to the gap pads in Figure 8b, the figure also shows that both gap fillers, regardless of thermal conductivity or module configuration, were superior in heat removal to the best-performing gap pad. Specifically, even the 2 W/m·K gap filler with extra shims removed more heat from the battery cells than the 4 W/m·K gap pad without shims. Also, the non-conformance of both gap pads resulted in much worse performance when shims were added, whereas there was very little difference between the two configurations with the gap fillers.

In addition to measurements of heat removed, we also assessed the battery module temperature performance in two ways. First, temperature data from the thermocouples attached to the individual cells were analyzed. Figure 9 shows time plots of the individual thermocouple readings from the top, middle, and bottom of each of the five battery cells, along with the averages of the five thermocouples in each position, for the two most extreme cases based on the previous plots. Figure 9a shows data for the 4 W/m·K gap filler with no extra shims, and Figure 9b shows data for the 4 W/m·K gap pad with shims. In both cases, the temperature was overall lowest next to the cooling plate (bottom) and highest at the lead end (top). There was a larger variation in individual temperature readings for the gap pad, and as expected the overall temperatures were higher for the gap pad, but the difference in maximum temperature between the gap filler and gap pad configurations was only about 4°C (about 43°C and 47°C, respectively), even though on a power basis these are the most extreme cases.

It should be noted that the thermocouples capture only the temperature on the outer side casings of the battery cells. The primary source of heat generation is inside the cell, however, and we have no knowledge of the thermal transfer properties of the cell interior. Much of the heat transfer may be occurring through the cell interior directly through the bottom of the cell, through the TIM and into the cold plate. We therefore devised a second experiment to calculate the bulk temperature of the battery module, T_i, at a particular time point, t_i, from the power measurements according to equation (2), where the first term in parentheses is the power removed from the battery cells (corrected for losses due to convection and the terminal leads), m is the mass of the battery, and Cp is the heat capacity of the battery determined by a drop calorimetry experiment.

$$T_i = (P_{battery} - P_{coolant} - P_{convection} - P_{leads}) * (t_i - t_{i-1}) / (m_{battery} * Cp_{battery}) + T_{i-1} \quad (2)$$

Figure 10 summarizes the calculated bulk temperature versus time for the various module configurations. In this figure, the lower values of temperature correspond to better thermal performance. As these values are derived from the heat-removed data in Figures 7-8, the results are qualitatively the same as discussed previously.

Figure 11 summarizes the average values for the peak temperatures determined using the two methods. In Figure 11a, the overall average peak cell temperatures determined from the combined temperature measurements from top, middle, and bottom thermocouples are plotted. The error bars represent the 95% confidence interval range for all temperatures and includes the variation between the top and bottom temperatures. Figure 11b is a plot of the peak temperatures from

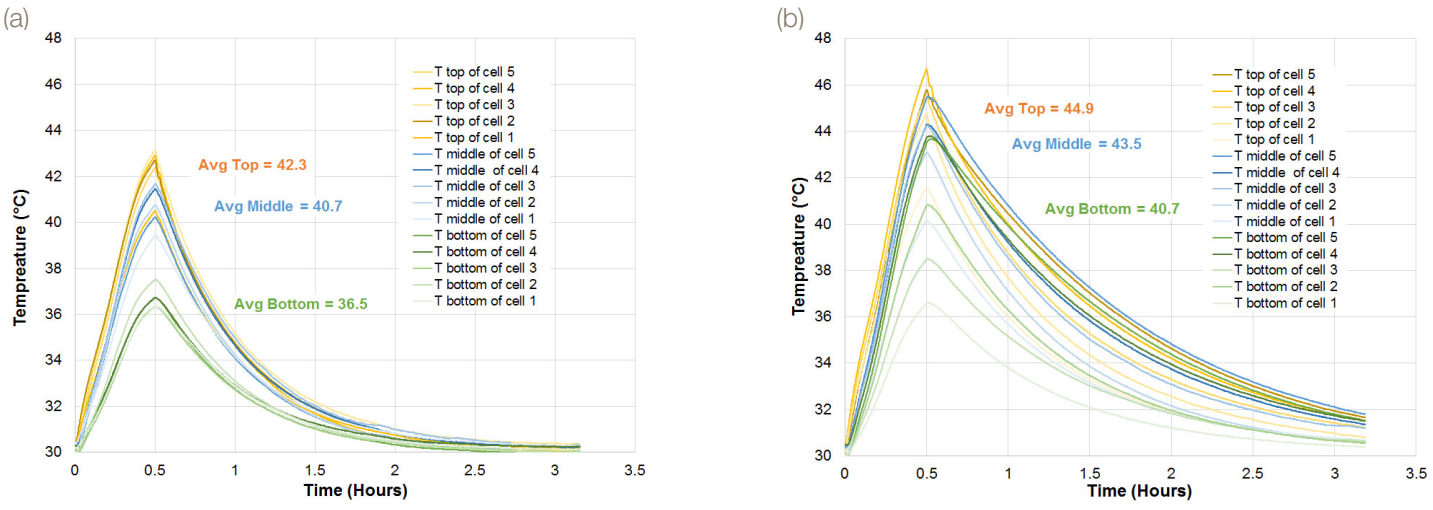

Figure 9: Comparison of cell thermocouple temperatures for (a) 4 W/m·K gap filler with no extra shims and (b) 4 W/m·K gap pad with shims. Individual curves for each of the five cells and average values for the top (orange), middle (blue) and bottom (green) thermocouples are shown.

the plots in Figure 10 and represents the global average battery cell temperature, including the entire cell rather than just the surface temperature. As expected, the bulk temperature is higher than the thermocouple temperatures, but the same general trends hold: the temperatures are lowest for the gap fillers, there is little overall difference between 2 and 4 W/m·K materials of a given type, and the effect of added shims is much less pronounced with the gap fillers versus the gap pads.

Conclusions

Our results show a clear advantage for liquid-dispensed gap fillers versus thermal gap pads for removing heat from and reducing temperatures in battery modules. Liquid-dispensed materials are able to fill irregular gaps due to surface roughness and also due to manufacturing irregularities to give uniform and repeatable performance in a full battery module. This is a practical demonstration of the fundamental findings in our previous white paper, which showed that the thermal impedance of gap fillers was much lower than gap pads due to a lower interfacial thermal resistance. With proper application, even a lower-conductivity gap filler can out-perform a higher conductivity gap pad.

Our results also show that you can gain excellent thermal performance even using a relatively low thermal conductivity gap filler. Higher conductivity gap fillers will become more valuable and more differentiated as the thermal load increases. In addition to the improved thermal performance, the ease and speed of application of CoolTherm liquid-dispense gap fillers makes them ideal for high-volume automotive manufacturing processes.

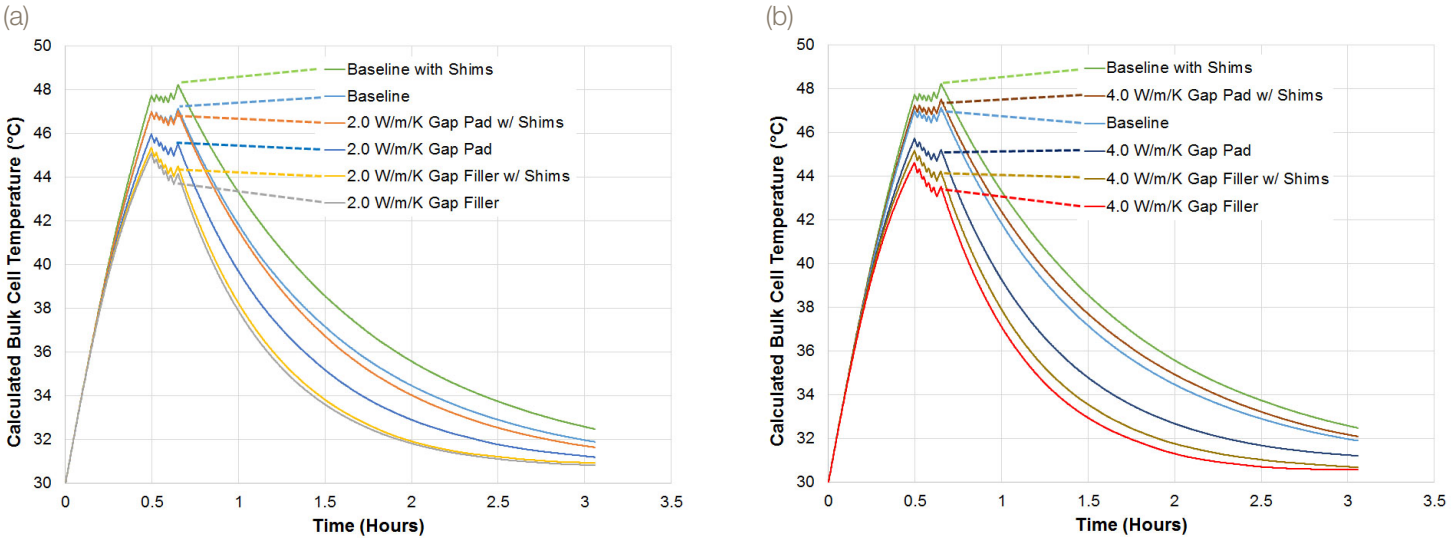

Figure 10: Comparison of calculated bulk cell temperature for modules using 2 W/m·K materials (a) and 4 W/m·K materials (b). Baseline had no thermal interface material.

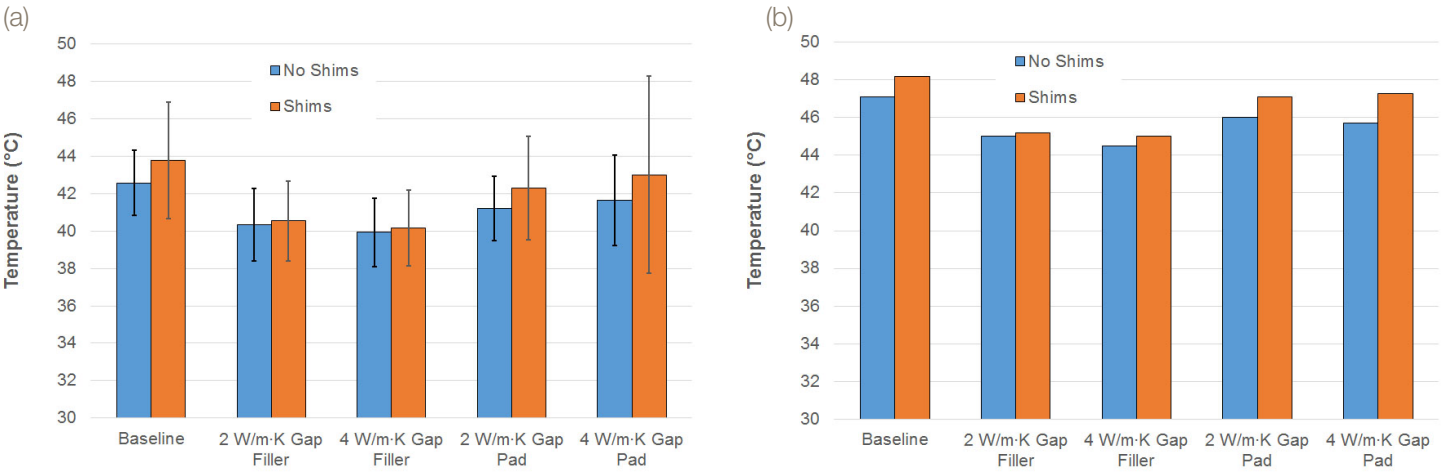

Figure 11: Overall average cell maximum temperatures based on averages of the individual thermocouple measurements (a) and bulk maximum cell temperatures calculated from calorimeter and power measurements (b) for the different cell module configurations. Error bars in Figure 11a correspond to 95% confidence intervals including measurements from the top, middle, and bottom of each cell.

Acknowledgments

We sincerely thank Matthew Keyser and Thomas Bethel at the National Renewable Energy Laboratory (NREL) in Denver, CO, for their invaluable assistance in planning, conducting, and analyzing the data for this study.

OD LL3250 03/20 Rev.1

Parker LORD
Engineered Materials Group

111 LORD Drive
Cary, NC 27511-7923
USA

phone +1 877 ASK LORD (275 5673)

www.lord.com